# Structure of Solid Poly(tetrafluoroethylene): A Computer Simulation Study of Chain Orientational, Translational, and Conformational Disorder

**Michiel Sprik**

*IBM Research Division, Zurich Research Laboratory, CH-8803 Rüschlikon, Switzerland*

**Ursula Röthlisberger**

*Physical Chemistry, ETH Zurich, CH-8092 Zurich, Switzerland*

**Michael L. Klein\***

*Department of Chemistry, University of Pennsylvania, Philadelphia, Pennsylvania 19104-6323*

*Received: October 25, 1996; In Final Form: January 7, 1997*[⊗]

The nature of the orientational, translational, and conformational disorder exhibited by poly(tetrafluoroethylene) has been characterized with the help of molecular dynamics calculations based on a new all-atom interaction potential function developed specifically for the perfluoroalkanes. The simulation has identified the following sequence of phenomena, which arise on heating the low-temperature crystalline phase: helical unwinding of chain segments, longitudinal jump diffusion of chains—without gauche defects—followed by generation of gauche defects. These observations accord well with experimental data.

## 1. Introduction

Solid poly(tetrafluoroethylene), PTFE, exhibits unique mechanical properties that form the basis for its numerous commercial uses as Teflon. The uniqueness of PTFE is linked to the occurrence of a polymorph, phase I, which has a remarkable thermal stability, ranging from 30 °C to the melting temperature at ∼330 °C. In phase I, the perfluoroalkane polymer chains are aligned parallel, in a close-packed structure. However, the orientations of individual $CF_2$ groups are only locally correlated and have no long-range order.[1,2] By contrast, in the crystalline solid, phase II, which exists below room temperature, the PTFE chains exhibit coherent helical winding with $n_\pi = 13$ $CF_2$ units in a 180° helix turn.[3,4] Soon after the identification of phase I by X-ray diffraction,[3] it was realized that the microscopic explanation for many of the properties of PTFE lies in the propensity of the polymer chains to disorder orientationally and translationally along the chain axis, well before melting. This behavior has its origin in the helical structure of perfluoroalkanes, which gives the individual polymer chains smooth outer contours with relatively little anisotropy for intermolecular interaction.

From studies of rotator phases of perfluoroalkane oligomers,[2] it is known that orientational disorder favors the formation of conformational defects. However, for a polymer the very existence of disorder depends on the coupling between conformation and orientation, and possibly translation as well. Accordingly, the thermally accessible rotational excitations of a polymer are confined to torsions of finite segments and, therefore, involve the creation of conformational defects. Moreover, correlation between inter- and intramolecular configurations necessarily plays an important role in the process of translational relaxation of the polymer. This, in turn, is the basis for the unique viscoelastic response in phase I, which, although a solid, flows more readily than the melt.[1] A characterization of the disorder in phase I of PTFE is, therefore, a precondition to the detailed understanding of its various macroscopic properties. Indeed, this was the motivation of several experimental studies aiming to elucidate the nature of PTFE.[4−8]

Phase I of PTFE has three regions of viscoelastic response: so-called $\gamma$-relaxation, which is interpreted as chain segment rotation and ranges from 160 K in the ordered solid phase II, through the phase transition, and up to roughly 400 K; $\beta$-relaxation, which is associated with the minimum in the NMR $T_{1c}$ around 450 K and speculated to involve longitudinal motion parallel to the chain axes, and $\alpha$-relaxation which involves anisotropic flow parallel to the molecular axes in the high-temperature solid. The mechanical behavior of phase I is such that at constant shear rate the shear stress first falls by an order of magnitude to reach a minimum around 500 K and then rises before melting. In the melt the viscosity is high due to chain entanglements.

Computer simulation and advanced graphical tools now provide a well-proven useful complement to available experimental techniques for the investigation of disorder in complex systems, because many of the relevant microscopic details can only be derived indirectly from ensemble-averaged experimental data.[9] Herein, the method of constant temperature−constant pressure molecular dynamics has been used to perform a numerical experiment on a realistic all-atom model of solid PTFE.[10]

## 2. Potential Model

Force field models for polymers usually make a distinction in the way inter- and intramolecular interactions are treated. However, the helicity of PTFE has been rationalized in terms of F atom "crowding".[3] The helical distortion of a hydrocarbon-like *all-trans* conformation and the anisotropic forces between $CF_2$ groups of adjacent chains have a common origin: the short-range repulsion of pairs of F atoms. Indeed, we have compared the conformational energies as determined for a set of perfluorobutane configurations by means of *ab initio* density functional methods[10] to F−F pair energies calculated from an empirical intermolecular interaction model for solid $CF_4$.[11] If the F−F

pair interactions of next nearest neighbor $CF_2$ and $CF_3$ groups (i.e., the atoms in 1−4, 1−5, and 1−6 positions) in $C_4F_{10}$ are subtracted from the corresponding *ab initio* total energies, the residual energies are found to be similar to a regular hydrocarbon-like dihedral potential profile[10] without additional minima for helical conformations. The 1−4 combinations favor a perfect *trans* (alkane-like) conformation. Hence, the repulsion between atom pairs in 1−5 and 1−6 positions can be identified as the interactions reponsible for the helical distortion. Accordingly, the residual energies were parametrized to yield a standard three-parameter dihedral potential function with a single *trans* and two equivalent *gauche* minima.[13] With exclusion of 1−2, 1−3, and 1−4 intramolecular interactions but including the 1−5 and 1−6 coupling using the empirical 12−6 F−F pair potentials of ref 11 this comparatively simple model is able to reproduce the four main conformational states of fluorocarbons. The identical 12−6 potentials were adopted to describe the interchain interactions. Another important aspect of the model is that C−C bond lengths and the C−C−C and C−C−F bond angles are treated as flexible molecular degrees of freedom. A similar approach has been used recently for the modeling of fluoropolymers in ref 14.

### 3. Molecular Dynamics Calculations

The present simulation utilizes the Parrinello−Rahman constant temperature−constant pressure molecular dynamics (MD) scheme in which the simulation box is allowed to change its dimensions due to thermal stresses. The number of independent PTFE chains in the periodically replicated MD box is 30. The choice of system size in the *c* direction is an important issue in the specification of a PTFE model. The number of $CF_2$ groups connected in a chain in the MD box should be commensurate with $n_\pi$, the number of $CF_2$ groups in a unit cell of the helical phase, and should span several of these unit cells. A complication is that the exact period of the helices in the crystal depends on the packing of the PTFE chains and on temperature. Experimental evidence for this dependence comes from the composite nature of the II−I transition: Before disordering at 30 °C, the phase II PTFE structure transforms at 19 °C to an intermediate phase IV in which the chains are slightly uncoiled. The number of $CF_2$ groups per 180° turn of the helix is increased from $n_\pi = 13$ to $n_\pi = 15$.[4,8] Normalized by the number of $CF_2$ groups, the energy differences for variation of $n_\pi$ by one or two units is extremely small (∼0.2 kJ mol$^{-1}$). The correct ordering of the ground state is very hard to reproduce in model calculations, and the uniform helical structure with minimum energy in our model turns out to be the one shown in Figure 1A, which has $n_\pi = 17$. The simulation box contained chains six times longer, i.e., with 102 $CF_2$ groups. Thus, the PTFE sample shown in Figure 1, which is the complete simulation box, contains about 9000 atoms. The use of a parallel architecture computer enabled us to follow the evolution of this system for a total duration of ∼6 ns. Further technical details of the MD simulation will be published elsewhere.[13]

Starting with a low-temperature, fully-ordered helical phase II structure, the system was heated in small steps ($\Delta T = 10$ or 20 K) up to the temperature where it attempted to melt (∼725 K). At around 575 K, an order−disorder transition to a phase I structure was observed at which the long-range orientational order perpendicular to the chain direction disappeared and, simultaneously, the coherence of the helical winding along polymer chains. The fluctuations responsible for the breakdown of the order were identified as small-angle torsional excitations. The local orientational correlations in the phase I structure that

remain above the observed transition are short helical portions, reminiscent of the fully ordered phase. Disordered phase I was found to be virtually free of gauche defects. Initially, the average positions of the $CF_2$ units are ordered. In spite of this crystalline translational order, we detected the occurrence of longitudinal jump diffusion, along the chain direction, on a nanosecond time scale.

Selected examples of structures generated in the MD simulations are given in Figure 1. A configuration sampled from the trajectory of the ordered phase II system at a temperature of 200 K is given in Figure 1A.[15] Two of the chains are highlighted by drawing atoms with van der Waals radii in order to give a clearer impression of the thermal fluctuations, which are mostly small-angle torsional defects. The long-range order is preserved, as can be seen from the skeleton pattern of the other chains. However, the number of orientational defects is already significant, even at this relatively low temperature. These seemingly contradictory observations can be reconciled if we assume that the defects along a chain are correlated.[16] On approaching the disordering phase transition, this correlation is weakened and, in turn, ultimately results in a breakdown of the long-range order. The phase I configuration shown in Figure 1B is consistent with this view. Long-range orientational order is lost in this state. However, although the concentration of defects is considerably larger than in phase II, the nature of the defects is very similar to the perturbations of helicity shown in Figure 1A for phase I.

### 4. Discussion

The picture of the II−I phase transition that emerges from the MD simulation (Figure 1A,B) is basically that of a continuous order−disorder transition. A quantitative analysis in terms of correlation functions of various structural properties demonstrates that on a length scale of approximately five $CF_2$ units the chains in phase I retain a largely helical conformation. The sudden collapse of the long-range coherence of the helical winding in phase II can be illustrated by the correlation in the orientation of the individual $CF_2$ units, probed at various points along a single chain. This correlation can be quantified by a function depending on the coordinates of the carbon atoms only. Indicating the position vector of the *m*th C atom in the *i*th polymer chain by $\mathbf{r}_{i,m}$ we define a single-chain conformational correlation function by the expression

$$C(n) = \frac{1}{N}\sum_i\sum_m (-1)^m \frac{\mathbf{d}_{i,m}\cdot\mathbf{d}_{i,m+n}}{d_{i,m}d_{i,m+n}} \qquad (1)$$

The vector $\mathbf{d}_{i,m} = \mathbf{r}_{i,m+1} + \mathbf{r}_{i,m-1} - 2\mathbf{r}_{i,m}$ is the bisector of the pair of C−C bonds joined by the *m*th C atom. $N$ is the total number of C atoms in the MD sample. The function $C(n)$ is plotted in Figure 2 for a series of thermodynamic states. The almost perfect harmonic curve for the 200 K state in Figure 2A confirms that defects, which are obviously present in the ordered phase, have little effect. However, close to the II−I transition (Figure 2B), damping of the harmonic behavior sets in. The damping of the function $C(n)$ becomes critical at the transition, which because of superheating[17] occurs at a much higher temperature (575 K) in the model than in experiment (Figure 2C). In the high-temperature phase I the orientational correlation exhibits a regular exponential decay (Figure 2D).

The function $C(n)$ in eq 1 measures the order along the chain direction. A similar function can be defined that is sensitive to correlations in the transverse direction, i.e., the degree of alignment of the monomeric units in a basal plane belonging to different chains. A convenient choice for the vectors in a
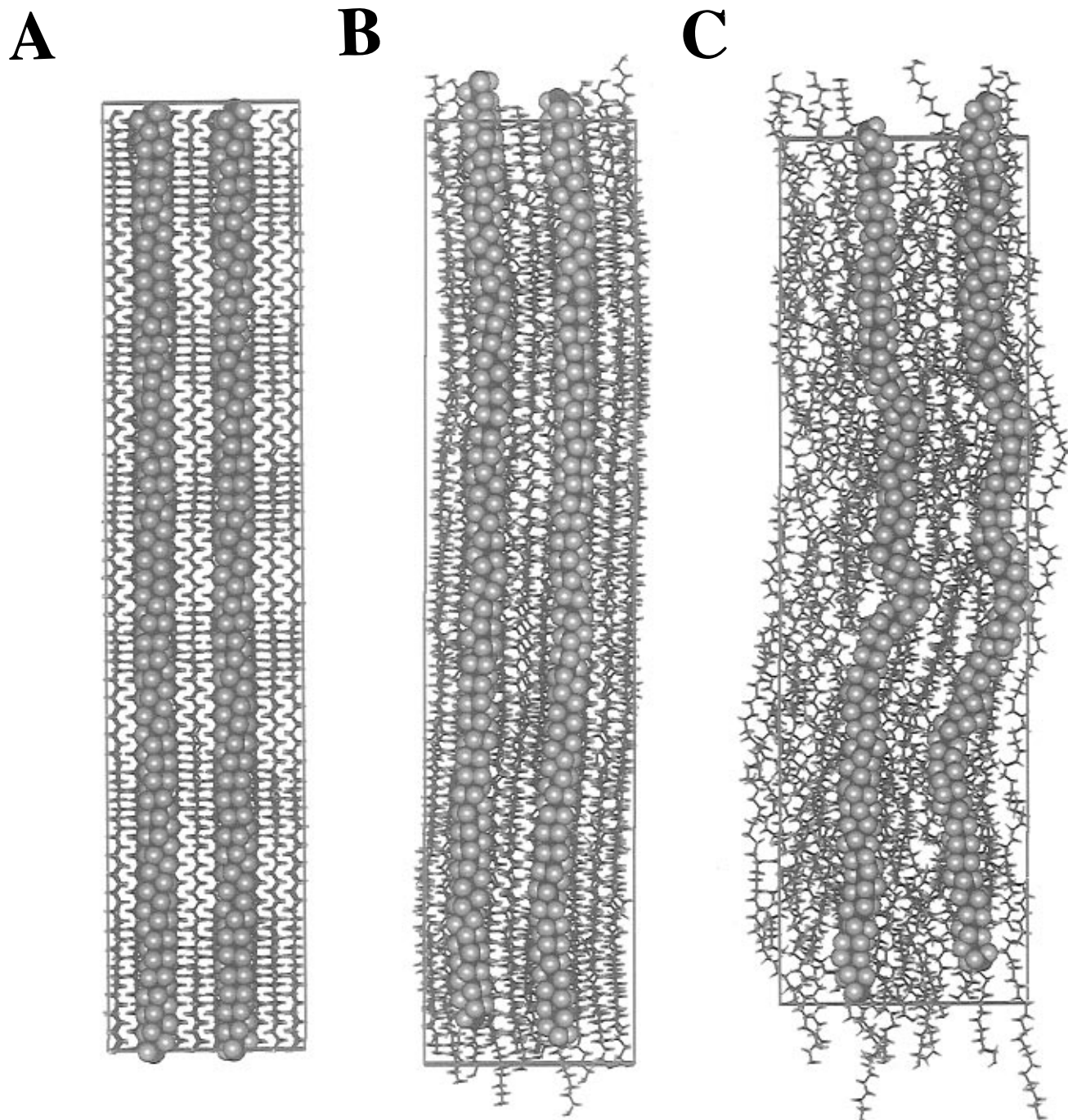
Letters

*J. Phys. Chem. B, Vol. 101, No. 15, 1997* **2747**

# A

# B

# C



**Figure 1.** Instantaneous configurations taken from the present MD simulation study of solid poly(tetrafluoroethylene). (A) The low-temperature (phase II, $T = 200$ K) state of the system viewed along the crystal $b$-axis. Here, $b \approx 3^{1/2} a$, and $a \approx 5.5$ Å is the nearest neighbor distance in the quasi hexagonal lattice formed by the perfluoroalkane polymer chains: fluorine atoms are blue; carbon atoms black. Two selected chains are rendered in a space-filling ball representation in which the individual atoms are asigned their appropriate van der Waals radii. (B) Disordered phase I at $T = 625$ K and (C) superheated phase I at $T = 895$ K. The three configurations are drawn on the same length scale in order to compare the dimensions of the MD box (red lines) at different temperatures.

scalar product similar to eq l is the symmetry axes of $CF_2$ groups indicated by $\mathbf{u}_{i,m}$, where the index $m$ labels again the units along a given chain $i$. Because of the helicity, the orientation of $\mathbf{u}_{i,m}$ varies with the longitudinal position of the plane, and an average of the cosines over the full sample will vanish even in a state of perfect orientational order. Hence, averaging is limited to $CF_2$ groups in thin slabs perpendicular the $c$-axis. The C atom positions in such a slice satisfy the condition $h_{ij} = c^{-1}\mathbf{c} \cdot (\mathbf{r}_i - \mathbf{r}_j) \leq w$, where we have suppressed the chain unit index $m$ in the position vectors $\mathbf{r}_i$ of the carbon atoms. $w$ is the width of the slab. By summing the scalar products of $\mathbf{u}_i$ and $\mathbf{u}_j$ over cylindrical shells, we can express the lateral orientational pair

correlation as a function of the projection $l_{ij} = r_{ij} - h_{ij}$ of $\mathbf{r}_{ij} = \mathbf{r}_i - \mathbf{r}_j$ on the basal plane

$$D(l) = \frac{1}{Ng(l)} \frac{d}{dl} \left[ \sum_{i,j} \theta(h_{ij}-w)\, \theta(l_{ij}-l) \frac{\mathbf{u}_i \cdot \mathbf{u}_j}{u_i u_j} \right] \quad (2)$$

where $\theta(x-a) = 1$ if $x \leq a$ and zero otherwise. $g(l)$ is a normalization factor obtained from an expression similar to eq 2 omitting the direction cosines. In practice, the value of $w$ is chosen such that all six nearest neighbors in a basal plane are included in the slab (for further technical details, see ref 13).
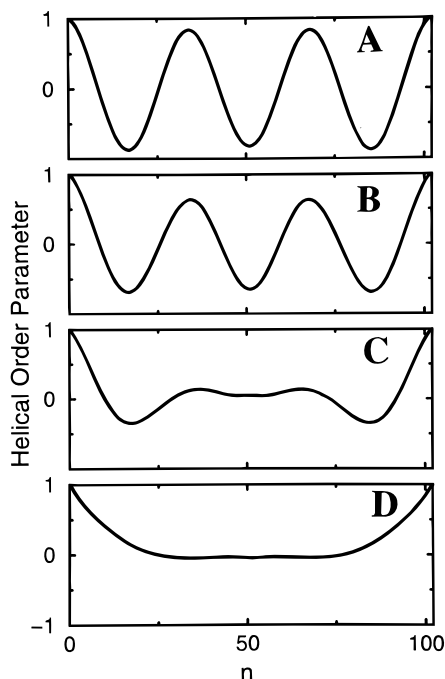
**Figure 2.** Correlation function monitoring the ensemble-averaged polymer chain helicity at different temperatures. The function shown correlates the cosines of the angle between the bisectors of pairs of adjoining carbon−carbon bonds of the polymer backbone as a function of the position *n* in the chain (for the precise definition, see eq 1. (A) The low-temperature function, i.e., phase II for the model, which exhibits three complete helical turns comprising the 102 $CF_2$ units that are contained in the periodically replicated MD simulation cell. (B), (C) and (D) show the effect of increasing temperature. The harmonic correlation in phase II (A) decays as a function of the $CF_2$ group index *n* along the polymer chain, to become a simple exponential in the disordered phase I (D). The temperatures at which the four correlation functions (A−D) were evaluated are those indicated by the open circles in Figure 3.
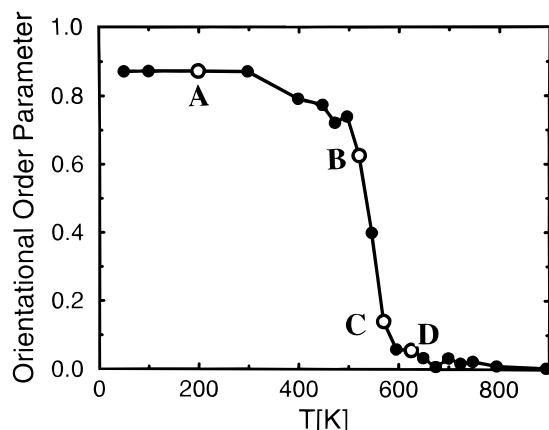


**Figure 3.** Interchain orientational order parameter for $CF_2$ groups as a function of temperature. The order parameter is defined as the average of the cosines of the angles between the bisectors of $CF_2$ groups of different chains contained in a thin slab perpendicular to the polymer direction (for the precise definition, see eq 2. The open circles correspond to the thermodynamic states for which Figure 2 gives the persistence of chain helicity. The orientational correlation between adjacent chains disappears between points C and D, i.e., in the same temperature interval as the coherence of the helical winding of the $CF_2$ units is lost (see Figure 2).

Figure 3 shows *D*(*l*) sampled at $l = l_c = 13$ Å as function of temperature. A value of $l_c = 13$ Å is close to the largest radial cutoff distance compatible with the limited lateral dimensions of our MD box. As is evident form Figure 3, the long-range

orientational order abruptly vanishes at the same temperature as the long-range persistence of helices is lost (Figure 2).

Gauche defects are almost absent in the phase I configurations produced by the simulation. Unlike the small-angle helical defects in Figure 1A,B, gauche defects would seriously distort the overall structure since they lead to the formation of kinks. However, gauche defects rapidly accumulate with further increase of temperature. This is accompanied by a lateral expansion of the sample and a contraction in the direction along the chains, which then start to meander as can be seen from the snapshot of the system at 895 K shown in Figure 1C. We interpret the change the simulation system is undergoing at 725 K as the onset of melting for the model, which is higher than the experimental melting point of about 610 K due to superheating.[17] Up to the melting temperature, the $CF_2$ groups are organized in more or less well-defined layers (sheets) perpendicular to the chain axis. In the simulation, this stacking becomes unstable around 725 K. Indeed, experimentally, the melting transition is evident from the temperature dependence of the layer lines in the structure factor.

The disorder in phase I induces both orientational and translational diffusive motion. The translational diffusion is highly anisotropic and preserves the layering of the $CF_2$ groups. It can be described as collective displacement of $CF_2$ groups along the chain direction. The effect of such fluctuations is particularly striking when the system is displayed without application of periodic boundary conditions (see Figure 1). The distance over which a polymer chain has moved in the course of the MD run is visible as a chain segment protruding from the MD box. An accumulative displacement of the size shown in Figure 1B (approximately five $CF_2$ units) is the result of 1 ns of simulation in phase I. During a comparable period of time spent in phase II such translational diffusion is negligible.[17]

In summary, the simulation described herein has identified the following sequence of phenomena, which arise on heating an idealized model of phase I of PTFE: helical unwinding of chain segments, longitudinal jump diffusion of chains−without gauche defects−followed by generation of gauche defects. The latter observation offers an explanation of why the viscoelastic response of PTFE is a minimum before the onset of melting. The generation of gauche defects appears to be a prelude to melting. These defects inhibit the motion of chains past each other, and thus their presence explains the rise in the viscosity. Ultimately, in the melt, chain entanglement will follow, but this is beyond the capabilities of the present simulation.

**References and Notes**

(1) Wunderlich, B.; Möller, M.; Grebowicz, J.; Bauer, H. *Adv. Polym. Sci.* **1988**, *87*, 50.

(2) Schwickert, H.; Strobl, G.; Kimmig, M. *J. Chem. Phys.* **1991**, *95*, 2800, 2807. For hydrocarbons, see e.g.: Sirota, E. B.; King, H. E., Jr.; Singer, D. M.; Shao, H. H. *J. Chem. Phys.* **1993**, *98*, 5809.

(3) Bunn, C. W.; Howels, E. R. *Nature* **1954**, *174*, 549.

(4) Clark, E. S.; Muus, L. T. *Z. Kristallogr.* **1962**, *117*, 119.

(5) Clark, E. S. *J. Macromol. Sci., Phys.* **1967**, *B1*, 795.

(6) McCall, D. W.; Douglass, D. C.; Falcone, D. R. *J. Phys. Chem.* **1967**, *71*, 998.

Letters

*J. Phys. Chem. B, Vol. 101, No. 15, 1997* **2749**

(7) Lathrop D. A.; Gleason, K. K. *Macromolecules* **1993**, *26*, 4652.

(8) Kimmig, M.; Strobl, G.; Stühn, B. *Macromolecules* **1994**, *27*, 2481.

(9) Ryckaert, J.- P.; Klein, M. L.; McDonald, I. R. *Mol. Phys.* **1994**, *83*, 439.

(10) Röthlisberger, U.; Laasonen, K.; Klein, M. L.; Sprik, M. *J. Chem. Phys.* **1996**, *104*, 3692.

(11) Nosé, S.; Klein, M. L. *J. Chem. Phys.* **1983**, *78*, 6928.

(12) Röthlisberger U.; Klein, M. L. *Chem. Phys. Lett.* **1994**, *227*, 390.

(13) Sprik, M.; Röthlisberger, U.; Klein, M. L. Manuscript in preparation.

(14) Holt, D. B.; Farmer, B. L.; Macturk, K. S.; Eby, R. K. *Polymer* **1996**, *37*, 1847.

(15) The assumption of a *uniform* helical ground state is a simplification since the experimental ground state consists of a mixture of right- and left-handed helices. In refs 5 and 8 it is argued that the average zero helicity of a bulk sample is achieved by organizing chains segments with equal handedness in domains separated by dislocation planes consisting of helix reversal defects. At low temperature the characteristic distance between these planes is at least as large as the length of a chain in our simulation.

(16) In ref 8 it is suggested that this correlation takes the form of coherent pairs of helix reversal defects. The distribution of defects in our simulation appears to be more disordered.

(17) In order to obtain an estimate of the effect of possible nonequilibrium states, we cooled the system again at the same rate as it was heated starting from a state just before the system displayed the first signs of melting. The phase I energies, lattice parameters, and dynamical properties were reproduced with satisfying accuracy. However, the spontaneous reestablishment of long range orientational order occurred at considerably lower temperature (425 K) compared to the disordering upon heating (575 K). This 150 K hystersis gives an estimate of the effect of superheating (and undercooling) that is caused by the rate of heating (cooling) used in the simulation. For similar reasons the onset of melting is observed at a higer temperature than the thermodynamic melting point of our model. Experimentally, the disordering transition occurs around room temperature. Finite-size scaling effects and deficiencies in the potential model are the likely cause of the higher transition temperature. These issues will be explored in more detail in ref 13.